

Optical Readout of Gold Nanoparticle-Based DNA Microarrays without Silver Enhancement

Gerhard A. Blab,* Laurent Cognet,* Stéphane Berciaud,* Isabelle Alexandre,† Dieter Husar,† José Remacle,† and Brahim Lounis*

*Centre de Physique Moléculaire Optique et Hertzienne–CNRS UMR 5798 et Université Bordeaux I, 33405 Talence Cedex, France; and †Eppendorf Array Technologies, 5000 Namur, Belgium

ABSTRACT We present a novel readout scheme for gold nanoparticle-based DNA microarrays relying on “Laser-Induced Scattering around a NanoAbsorber”. It provides direct counting of individual nanoparticles present on each array spot and stable signals, without any silver enhancement. Given the detection of nanometer-sized particles, which minimize the steric hindrance, the linear dynamic range of the method is particularly large and well suited for microarray detection.

Received for publication 14 October 2005 and in final form 3 November 2005.

Address reprint requests and inquiries to Brahim Lounis, E-mail: b.lounis@cpmoh.u-bordeaux1.fr.

The determination and exact quantification of gene expression is becoming increasingly important in basic pharmaceutical and clinical research. Fluorescence-based DNA assays are most widely used, but suffer from the presence of autofluorescence in some biological samples and substrates, which severely interferes with the detection of the target molecules. DNA assays based on gold nanoparticle (AuNP) labels present a viable alternative. They commonly use AuNPs larger than 40 nm, which can be readily detected due to their strong light scattering at visible wavelengths (1,2). For increased specificity and reactivity, AuNPs smaller than 40 nm are preferred. Indeed, small AuNPs functionalized with oligonucleotides exhibit a very sharp thermal denaturation profile, and the rate of reaction on a surface is much higher than with large particles (3–5). As small AuNPs (diameter <40 nm) barely interact with light, their direct optical detection has been impossible until recently without silver staining enhancement techniques (3,5). However, saturation at the amplification step limits the linear dynamic range as the typical size of the silver crystals is much larger than that of the AuNPs (4). Furthermore, spontaneous conversion of silver solution into metallic grains can occur leading to nonspecific signals (4). Another alternative is the electrical detection of the AuNPs after catalytic or enzymatic deposition of the silver (6–8).

Recently, the optical detection of AuNPs smaller than 40 nm as been achieved by photothermal detection methods (9,10). The most simple and sensitive one (10) relies on “Laser-Induced Scattering around a NanoAbsorber” (LISNA) and allows for the unprecedented detection of AuNPs smaller than 2 nm. We show here that by applying LISNA for the optical readout of small AuNPs in DNA microarrays, one can avoid the silver enhancement step and its drawbacks.

The experimental setup uses a combination of a time-modulated heating laser beam (close to the plasmon resonance of Au, e.g., at 514 nm or 532 nm with <1 mW power modulated at $\Omega \sim 300$ kHz) and a nonresonant probe

beam (633 nm, HeNe laser) (Fig. 1 *a*). The heating induces time-modulated variations of the refraction index around the absorbing AuNP. The interaction of the probe beam with this index profile produces a scattered field with sidebands at $\pm\Omega$. The scattered field is then detected through its beatnote with the probe field, which plays the role of a local oscillator as in any heterodyne technique and is extracted by lock-in detection. Two-dimensional raster scanning of the beams with galvanometric mirrors allows obtaining images of the samples.

In this study, we used standard low-density spotted DNA microarrays. These arrays are well suited for routine applications as they contain a limited number of genes (usually below 1000), which enables good spotting quality and good reproducibility (11). The test arrays were composed of serial dilutions of biotinylated capture probes having a length of 415 bases aminated in their 5' end. The capture probes were synthesized by polymerase chain reaction having one primer aminated at the 5' end. Biotinylated dCTP and dATP were incorporated during the polymerase chain reaction synthesis. Amplicons were purified to remove the excess dNTP and primers, and were spotted on aldehyde-activated slides. Anti-biotin/gold (20 nm) conjugates were used (BBInternational, Cardiff, UK). The concentrations corresponded to the full dynamic range afforded by silver staining enhancement imaging. Each row of the array consisted of one concentration spotted in quintuplet (Fig. 1 *b*).

For each spot of the microarray, we performed LISNA images with two different resolutions. In the “low resolution regime”, $200 \times 200 \mu\text{m}^2$ images were acquired with step sizes of $2 \mu\text{m}$, twice the size of the laser focal spot. In this condition, a fast scanning of entire spots is achieved but at the cost of subsampling the surface. In the “counting regime”, only a small (central) portion of the spots is

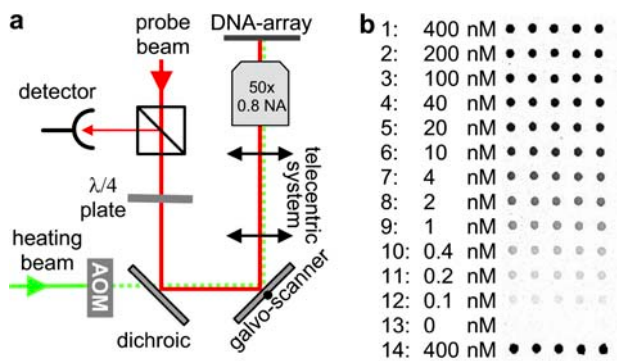


FIGURE 1 (a) Experimental setup (see text). AOM: acousto optics modulator. Integration time: 20 ms per point; heating intensity: ~ 100 kW/cm² on the sample. (b) Microarray layout imaged after silver staining enhancement.

scanned ($20 \times 20 \mu\text{m}^2$ images, $0.2 \mu\text{m}$ per point). The high resolution of the counting regime ultimately allows for detecting all individual AuNPs.

Low resolution images of four different spots are presented in Fig. 2 a. Regions of total coverage of the surface are found (spots 1–4), in which the outlines of the spots are

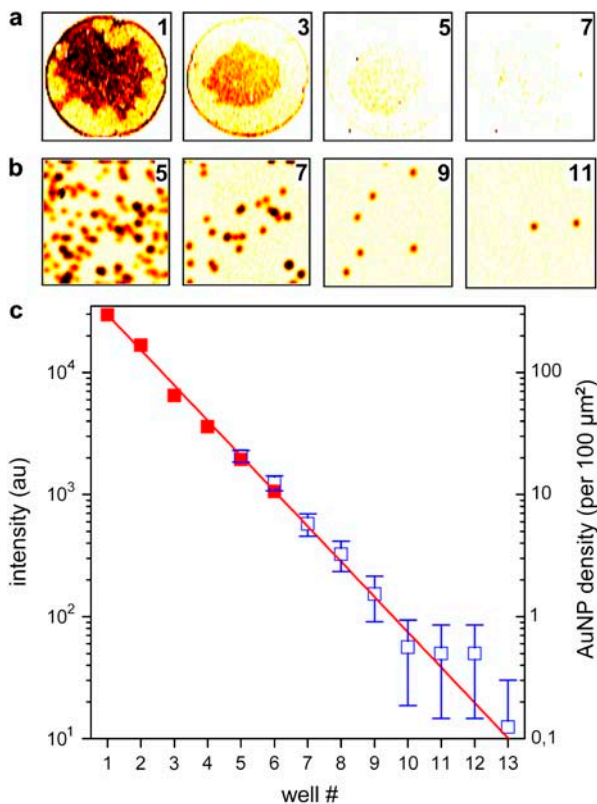


FIGURE 2 Direct imaging (no silver enhancement) of four spots by LISNA in the low resolution (a) and counting regime (b). (c) Signal versus well number in the low resolution (■) and counting regime (□).

clearly visible (12). For those, the average distances between AuNPs are smaller than the scanning resolution that corresponds to a surface density of AuNPs greater than typically one per $1 \mu\text{m}^2$. From these images, an average signal per spot is extracted. It gives a precise quantification of the amount of hybridization that occurred in the spots (Fig. 2 c, *solid squares*). A linear variation of the signal is obtained for a concentration range of ~ 2 logs with no deviations from linearity on the high labeling concentrations side. When the density of AuNPs is smaller than one particle per squared pixel size (spots 7 and greater), we switched to the counting regime so that all individual particles are detected and resolved (Fig. 2 b). The results given by the low resolution recordings are thus extended at least by 1 decade in the low concentration region by adding the mean density of individual AuNPs detected in the counting regime (Fig. 2 c, *open squares*), at the cost, however, of longer measurement times as the resolution was increased 10 times. Note that images obtained with the two resolutions lead to identical quantifications for the intermediate spots (5 and 6).

Our method provides a reliable quantification of the amount of DNA molecules in each spot of the microarrays, and three logs of linear signal were obtained (the full range of the tested arrays); this determination is no longer limited by any constraints of the detection method, but only by the degree of unspecific signals on one side and by the size of the AuNPs on the other side. Indeed, as all AuNPs are detected, the lower detection of DNA only depends on unspecific DNA hybridization events and on the quality of surface treatments (12). Concerning the upper detection limit, the ultimate limit is given by the condition of weak plasmon coupling between particles. Indeed, when the average distance of the AuNPs is comparable to their size, the optical response of AuNPs is modified (13). The theoretical dynamics thus represents more than 4 decades of signal with 20 nm AuNPs and scanning areas of $20 \times 20 \mu\text{m}^2$ as used here. Furthermore, the possibility to detect much smaller AuNPs (down to 1.4 nm) (10) by LISNA should significantly increase the dynamic range.

In addition to the high sensitivity and dynamics afforded by the use of LISNA, AuNPs-based DNA arrays can be stored for long periods and measured several times. Our approach thus combines the advantages of fluorescence measurements—small marker size, purely optical detection—with the high stability, specificity, and dynamic range afforded by AuNP labeling techniques. This makes LISNA a promising approach for application in biochips.

ACKNOWLEDGMENTS

G.A.B. acknowledges financial support by Fonds zur Förderung der wissenschaftlichen Forschung (FWF, Austria, Schrödinger-Stipendium) and the Fondation pour la Recherche Médicale (FRM, France). This research was funded by Centre National de la Recherche Scientifique (ACI Nanoscience and DRAB), Région Aquitaine, and the French Ministry for Education and Research (MENRT).

REFERENCES and FOOTNOTES

1. Yguerabide, J., and E. E. Yguerabide. 1998. Light-scattering sub-microscopic particles as highly fluorescent analogs and their use as tracer labels in clinical and biological applications. *Anal. Biochem.* 262:137–156.
2. Schultz, S., D. R. Smith, J. J. Mock, and D. A. Schultz. 2000. Single-target molecule detection with nonbleaching multicolor optical immunolabels. *Proc. Natl. Acad. Sci. USA.* 97:996–1001.
3. Taton, T. A., C. A. Mirkin, and R. L. Letsinger. 2000. Scanometric DNA array detection with nanoparticle probes. *Science.* 289:1757–1760.
4. Alexandre, I., S. Hamels, S. Dufour, J. Collet, N. Zammateo, F. De Longueville, J. L. Gala, and J. Remacle. 2001. Colorimetric silver detection of DNA microarrays. *Anal. Biochem.* 295:1–8.
5. Fritzsche, W., and T. A. Taton. 2003. Metal nanoparticles as labels for heterogeneous, chip-based DNA detection. *Nanotechnology.* 14:R63–R73.
6. Park, S. J., T. A. Taton, and C. A. Mirkin. 2002. Array-based electrical detection of DNA with nanoparticle probes. *Science.* 295:1503–1506.
7. Möller, R., R. D. Powell, J. F. Hainfeld, and W. Fritzsche. 2005. Enzymatic control of metal deposition as key step for a low-background electrical detection for DNA chips. *Nano. Lett.* 5: 1475–1482.
8. Moreno-Hagelsieb, L., P. E. Lobert, R. Pampin, D. Bourgeois, J. Remacle, and D. Flandre. 2004. Sensitive DNA electrical detection based on interdigitated Al/Al₂O₃ microelectrodes. *Sens. Actuators B. Chem.* 98:269–274.
9. Boyer, D., P. Tamarat, A. Maali, B. Lounis, and M. Orrit. 2002. Photo-thermal imaging of nanometer-sized metal particles among scatterers. *Science.* 297:1160–1163.
10. Berciaud, S., L. Cognet, G. A. Blab, and B. Lounis. 2004. Photothermal heterodyne imaging of individual nonfluorescent nanoclusters and nanocrystals. *Phys. Rev. Lett.* 93:257402.
11. Zammateo, N., S. Hamels, F. De Longueville, I. Alexandre, J. L. Gala, F. Brasseur, and J. Remacle. 2002. New chips for molecular biology and diagnostics. *Biotechnol. Annu. Rev.* 8:85–101.
12. Festag, G., A. Steinbruck, A. Wolff, A. Csaki, R. Moller, and W. Fritzsche. 2005. Optimization of gold nanoparticle-based DNA detection for microarrays. *J. Fluoresc.* 15:161–170.
13. Sonnichsen, C., B. M. Reinhard, J. Liphardt, and A. P. Alivisatos. 2005. A molecular ruler based on plasmon coupling of single gold and silver nanoparticles. *Nat. Biotechnol.* 23:741–745.